

Integrating UAV and satellite data to assess the effects of agroforestry on microclimate in Dodoma region, Tanzania

Villani, Lorenzo
Department of Agriculture, Food,
Environment and Forestry (DAGRI)
University of Florence
Florence, Italy
lor.villani@libero.it

Castelli, Giulio
Department of Agriculture, Food,
Environment and Forestry (DAGRI)
University of Florence
Florence, Italy
giulio.castelli@unifi.it

Sambalino, Francesco
MetaMeta Research
Wageningen, the Netherlands
fsambalino@metameta.nl

Almeida Oliveira, Lucas Allan
Department of Agricultural
Engineering (DEA)
Federal University of Viçosa
Viçosa, State of Minas Gerais, Brazil
lucas11allan@hotmail.com

Bresci, Elena
Department of Agriculture, Food,
Environment and Forestry (DAGRI)
University of Florence
Florence, Italy
elena.bresci@unifi.it

Abstract— The present study investigates the microclimatic effect of trees in agroforestry systems in Dodoma region, Tanzania. A pixel-based analysis of Land Surface Temperature (LST) and Tree Canopy Cover (TCC) was performed on aerial imagery obtained with an Unmanned Aerial Vehicle (UAV) and on satellite data. UAV orthomosaic maps and satellite scenes were elaborated with a suite of Geographical Information Systems and the resulting data were statistically analyzed through linear regression, the Kruskal-Wallis test and the Dunn test. Results showed that the TCC of the surveyed areas was 5,1%, and a significant decrease in LST of 1,32 °C ($p<0,01$) was only found in areas with the highest TCC, during the late dry season. From these preliminary analyses, we suggest that a threshold of 10% TCC should be reached to have an ameliorated microclimate, in terms of temperature, in this agroecological zone. Considering the average plant phenotype characteristic to the area, it corresponds to a tree density of 50 trees per hectare.

Keywords—ecosystem restoration, microclimate management, meso-climate, agroforestry, UAV, Land Surface Temperature, Tree Canopy Cover

I. INTRODUCTION

In the framework of the Sustainable Development Goals, the UN launched the Decade for Ecosystem Restoration, to increase food security, improve livelihoods, conserve biodiversity and counteract the impacts of climate change, particularly in areas with high natural resources degradation.

Justdiggitt, an NGO committed to ecosystem restoration, is among those organizations that immediately joined the initiative. One of the intervention areas of Justdiggitt is the semi-arid region of Dodoma, Tanzania ($6^{\circ}11'S$; $35^{\circ}45'E$) (Fig. 1), that is affected by severe land degradation and consequent low productivity [1]. In 2017, in collaboration with the NGO LEAD Foundation, Justdiggitt started the “Regreening Dodoma Program” (RDP) to spread among farmers the Farmer Managed Natural Regeneration (FMNR) agroforestry system, to increase multipurpose tree density in farmlands and restore land and agroecosystems.

In order to develop an adequate knowledge of agroforestry systems in the area before upscaling FMNR intervention,

some areas within the RDP, representing typical agricultural landscapes with different tree densities, were selected (Fig. 1).

Trees outside forests are experiencing a renovated interest, and the improved mapping procedures and technologies provide interesting opportunities for new research to better understand their social, economic, and environmental role [2, 3].

Agroforestry systems are fundamental for ecosystem restoration as they provide multiple beneficial ecosystem services [4, 5]. Nonetheless, trees and crops also compete for water, nutrients and light resources and, to increase the rate of adoption by farmers, an appropriate set of agronomic practices is needed to reduce the trade-offs and enhance the complementarities [6, 7]. More research is therefore essential to better understand the dynamics of agroforestry systems at different scales, and an important aspect to be considered is the modification of the whole set of microclimate variables caused by the inclusion of trees into agroecosystems [8, 9].

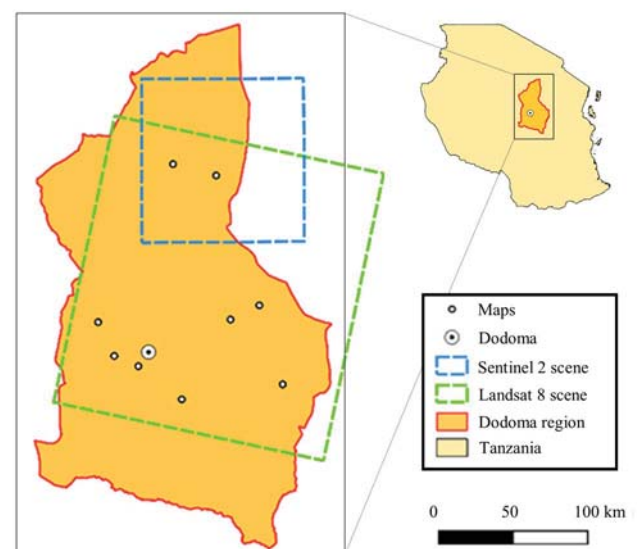


Figure 1: Study area: Dodoma region, Tanzania, with the borders of the Landsat 8 and Sentinel 2 scenes used and the locations of the selected study areas.

Microclimate, defined as the localized conditions of temperature, humidity, and atmosphere in the immediate vicinity of an organism, can be modified by farmers [10], and its management can play a major role as a form of adaptation to climate change [11, 12]. In agriculture, microclimate variables are generally studied implementing field experiments [13], while in this research a remote sensing methodology, including Unmanned Aerial Vehicle (UAV) and satellite data, was used.

Within the different microclimate variables, the research focused on soil temperature through the analysis of the remote-sensing retrieved variable Land Surface Temperature (LST), namely the temperature of the Earth surface, that can be approximated to the soil temperature of the first layer [14].

Trees are known to have a mitigating effect on extreme temperatures, lowering the maximum temperature due to reduced solar radiation during daytime, and increasing the minimum temperature due to reduced reflection of infrared radiation at night [8, 15]. At wider scales, research conducted on the urban heat island effect demonstrated the beneficial impact of tree density lowering the temperatures [16].

Within the wide framework of ecosystem restoration research, this study aims to deepen the knowledge of agroforestry systems dynamics, analysing their effects on microclimate through an innovative remote sensing approach that combine UAV and satellite data, to understand the potential impacts of the RDP and to suggest an operative tree density threshold to be set as objective.

II. MATERIALS AND METHODS

The LST of the selected areas was calculated for the dry season of 2018 (April – November). Among the various methods available to retrieve LST from satellite data, the Practical Single Channel (PSC) algorithm developed by [17] was selected because it is quite easy to be applied, it uses Landsat 8 and therefore has a good spatial resolution, and showed an improved performance compared to previous single channel algorithms [17].

The PSC algorithm retrieves LST through the following equations:

$$T_s = \frac{c_2 / \lambda}{\ln \left(\frac{c_1}{\lambda^5 \cdot B(T_s)} + 1 \right)} \quad (1)$$

$$B(T_s) = a_0 + a_1 w + (a_2 + a_3 w + a_4 w^2) \frac{1}{\epsilon} + (a_5 + a_6 w + a_7 w^2) \frac{1}{\epsilon} L_{\text{sen}} \quad (2)$$

Where T_s represents the LST, L_{sen} the at-sensor radiance ($\text{W} \cdot \text{m}^{-2} \cdot \text{sr}^{-1} \cdot \mu\text{m}^{-1}$), ϵ the emissivity (/), λ the effective wavelength (μm), that for band 10 equals $10.896 \mu\text{m}$ according to [18], w the Atmospheric Water Vapor (AWV) content ($\text{g} \cdot \text{cm}^{-2}$), $B(T_s)$ the Planck's radiance with a temperature of T_s , c_1 equals $1.19104 \times 10^8 \text{ W} \cdot \mu\text{m}^4 \cdot \text{m}^{-2} \cdot \text{sr}^{-1}$ and c_2 equals $1.43877 \times 10^4 \mu\text{m} \cdot \text{K}$, and $a_0, a_1, a_2, a_3, a_4, a_5, a_6, a_7$ are coefficients provided by the authors.

The emissivity was calculated through an NDVI threshold method, following the procedure proposed by [18], through the following equations:

$$\epsilon = \begin{cases} \epsilon_s & \text{NDVI} < \text{NDVI}_s \\ \epsilon_v \cdot P_v + \epsilon_s \cdot (1 - P_v) + C & \text{NDVI}_s \leq \text{NDVI} \leq \text{NDVI}_v \\ \epsilon_v + C & \text{NDVI} > \text{NDVI}_v \end{cases} \quad (3)$$

$$P_v = \left[\frac{\text{NDVI} - \text{NDVI}_s}{\text{NDVI}_v - \text{NDVI}_s} \right]^2 \quad (4)$$

$$C = (1 - \epsilon_s) \cdot \epsilon_v \cdot F' \cdot (1 - P_v) \quad (5)$$

Where NDVI_s and NDVI_v are the NDVI thresholds for soil and vegetation, respectively, individuated in the NDVI histograms of the Landsat 8 scenes considered for the research, ϵ_s and ϵ_v are the emissivity values for soil and vegetation, respectively, P_v is the fraction of vegetation, that must be set to zero for pixels with $\text{NDVI} < \text{NDVI}_s$ and set to one for pixels with $\text{NDVI} > \text{NDVI}_v$, C is the cavity effect, and F' is the geometrical factor, generally assumed equal to 0.55.

AWV was obtained from the value Total Water Vapor Column of the product MCD19A2 (Version 6) of MODIS, at a resolution of 1 km. Cloud-free Landsat 8 scenes (path 168, row 64) were used to calculate the NDVI with bands 4 and 5, and the LST with band 10. For further analysis, cloud-free Sentinel 2 scenes (Tile Number: T36MZV) with less than 10 days difference in the acquisition date from the corresponding Landsat 8 scenes, were used to calculate the NDVI, and consequently the emissivity, with bands 4 and 8, increasing the study resolution from 30m to 10m.

At the end of the dry season 2018 (November), a DJI Phantom Pro 4 UAV, equipped with a Parrot-Sequoia multispectral camera, was used to survey the surrounding areas of nine villages within the RDP, throughout the whole Dodoma region. The obtained imagery was processed using the photogrammetry software Agisoft Photoscan into nine Red-Green-Blue (RGB) and one NDVI orthomosaic maps. The surveyed areas were mostly representing farmland, with the inclusion of some small portions of natural vegetation (mainly bushlands and few patches of trees), urban areas (roads and houses), and sand rivers. Each orthomosaic map covered a swath of farmland with an average size of 50 hectares (700 m x 700 m).

Vectorial grids, with the same dimensions and positioning of the pixels of the Landsat 8 and Sentinel 2 scenes, were created and overlaid over the UAV orthomosaic maps (Fig. 2). A supervised classification of the orthomosaic maps was

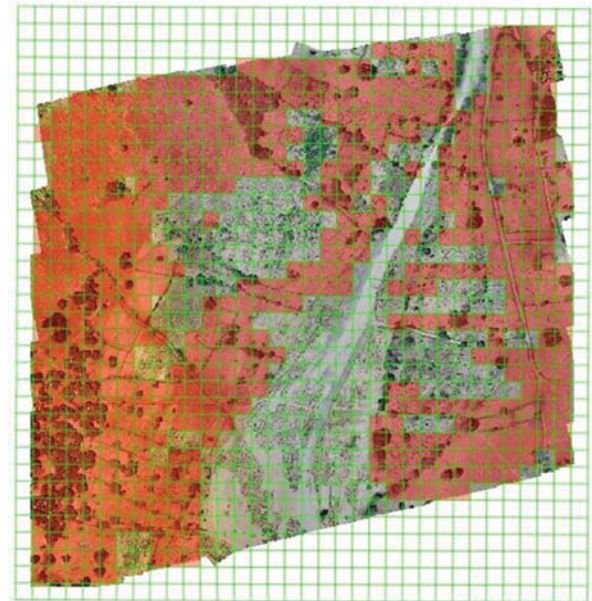


Figure 2: Landsat 8 vectorial grid overlaid over the UAV orthomosaic map of the greenest map. In red the cells selected for the analysis after the visual check.

then performed to identify trees and consequently calculate the Tree Canopy Cover (TCC) for each cell of the vectorial grid. A visual check was then performed, to exclude cells containing urban areas, bushlands, and rivers, and to manually digitize trees if the supervised classification was imprecise (Fig. 3).

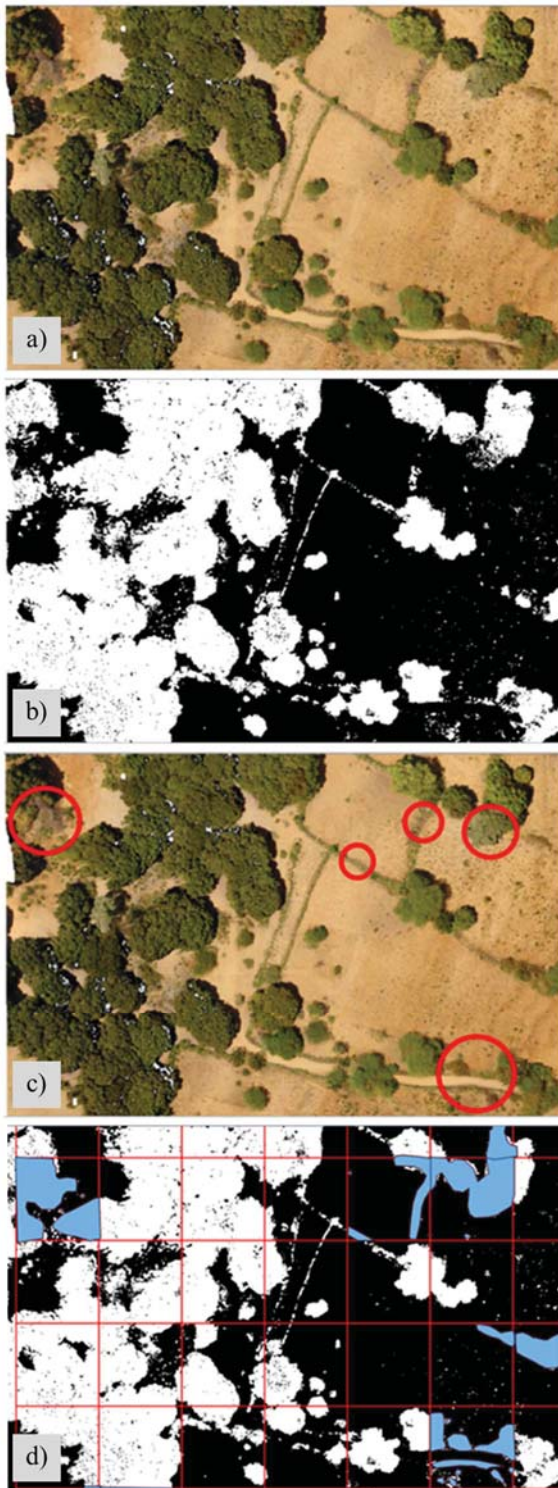


Figure 3: An example of the orthomosaic maps processing procedure: a) a portion of an orthomosaic map used for this research; b) the supervised classification (tree/no tree) obtained; c) the visual check phase, in which the errors of the supervised classification were spotted; d) the manual digitization of trees and bushes for the cells of the vectorial grid containing the errors of the supervised classification.

The correlation between LST and TCC was computed through a pixel-based analysis, considering the pixels individually at first, and through a class-based analysis then. In the class-based analysis, the pixels were grouped in five classes with 10% TCC increments and a maximum of 50% TCC.

Linear regressions were performed to verify if there was correlation between TCC and LST. The Kruskal-Wallis test was then applied to verify if the TCC classes were promoting statistically significant differences on the average LST. When the Kruskal-Wallis test was significant, the Dunn test was used to verify between which TCC classes the differences in LST were significant.

III. RESULTS

LST maps were retrieved through the PSC algorithm for the dry season of 2018 (two examples are shown in Fig. 4), and the orthomosaic maps were processed with the vectorial grid at 30m resolution to calculate the TCC, that averaged 5,1% (Tab. 1).

The LST/TCC correlation was analyzed for the individual orthomosaic maps considered, without aggregating them. Because of the low TCC, most of the orthomosaic maps did not show any relevant correlation between LST and TCC. The two orthomosaic maps with the highest TCC (TCC > 7,2%) revealed the expected correlation, and particularly the greenest one (TCC = 18,2%).

The pixel-based analysis yielded poor results, without any evident correlation between TCC and LST observed. Instead, results of the class-based analysis showed the expected negative correlation ($R^2 > 0,9$) for the two orthomosaic maps with the highest TCC for the late dry season (August – November).

The Kruskal-Wallis and Dunn tests were then applied to the two orthomosaic maps with the highest TCC, and consistent significant results were obtained only for the greenest orthomosaic map. More in detail, the LST of the 0-10% TCC class was found to be significantly higher ($p < 0,01$) compared to the all the other classes with higher TCC.

The NDVI map, available for the greenest orthomosaic map, was used to perform the supervised classification of trees

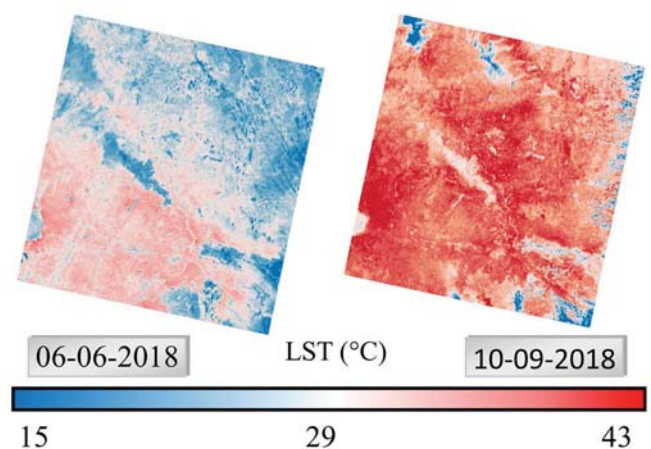


Figure 4: Land Surface Temperature (°C) of the Landsat 8 scenes retrieved through the Practical Single Channel algorithm, for the 6th of June 2018, and the 10th of September 2018.

Table 1: Tree Canopy Cover and number of cells of the vectorial grids created with Landsat 8 pixels for the nine orthomosaic maps studied.

Map	1	2	3	4	5	6	7	8	9	Total
TCC (%)	18,2	7,2	5,0	4,9	4,7	3,6	3,0	0,9	0,8	5,1
Number of cells	544	225	349	571	838	228	914	487	627	4783

at an increased resolution of 10m. The more precise classification allowed to skip the manual digitization part of the procedure, that would have been too much time-consuming considering the high number of cells.

The same statistical analyses were performed and yielded more significant results. In particular, the class-based analysis showed improved results in terms of linear regressions and level of significance of the Kruskal-Wallis and Dunn tests, with significant decreases in LST when comparing all the classes considered in the scenes of the late dry season. In Fig. 5 are shown the results of the class-based analysis of the greenest orthomosaic map, with the inclusion of the Sentinel 2 vectorial grid at 10m resolution.

The average difference in LST between the class with less trees (0-10% TCC) and the one with more trees (40-50% TCC), considering the late dry season (August – November), amounts 1,32 °C and it is statistically significant ($p < 0,01$).

IV. DISCUSSION AND CONCLUSION

The microclimate of agroforestry systems in Dodoma region was studied through a pixel-based analysis of LST and TCC, integrating satellite and UAV data, to understand the benefits of an increased tree density on temperature.

LST was retrieved with the PSC algorithm and TCC was calculated through a supervised classification of the UAV orthomosaic maps. The expected correlation was found only in the maps with the highest TCC during the late dry season, with a significant decrease in temperature of 1,32 °C ($p < 0,01$).

In most of the orthomosaic maps analyzed, no correlation between TCC and LST was found. It is important to point out that most of the orthomosaic maps had cells belonging to all the five TCC classes considered, but only for the orthomosaic map with the highest total TCC a strong correlation was found and the differences in LST were significant, meaning that the total TCC of the orthomosaic maps played a major role.

The poor results are also caused by the fact that tree density is not the only factor controlling LST; different kind of soils, vegetation cover, altitude, other microclimate conditions like soil moisture and wind exposure, agronomic practices like soil tillage and mulching, among others, can be all considered as confounding factors that have a localized influence on LST. Probably, meso-climate characteristics of the surrounding areas also play a role. Regarding trees, it is likely that the phenotype characteristics of the species have a different effect on temperature. Higher trees with more shade have an increased impact on temperature, as well as trees compared to bushes, and evergreen trees are better contributor compared to deciduous.

In this research, to limit the impact of the confounding factors, a large study area was considered, with a total of 4783 30x30 m cells (430 hectares). A similar reflection can be made for the reasons behind the fact that the increased resolution

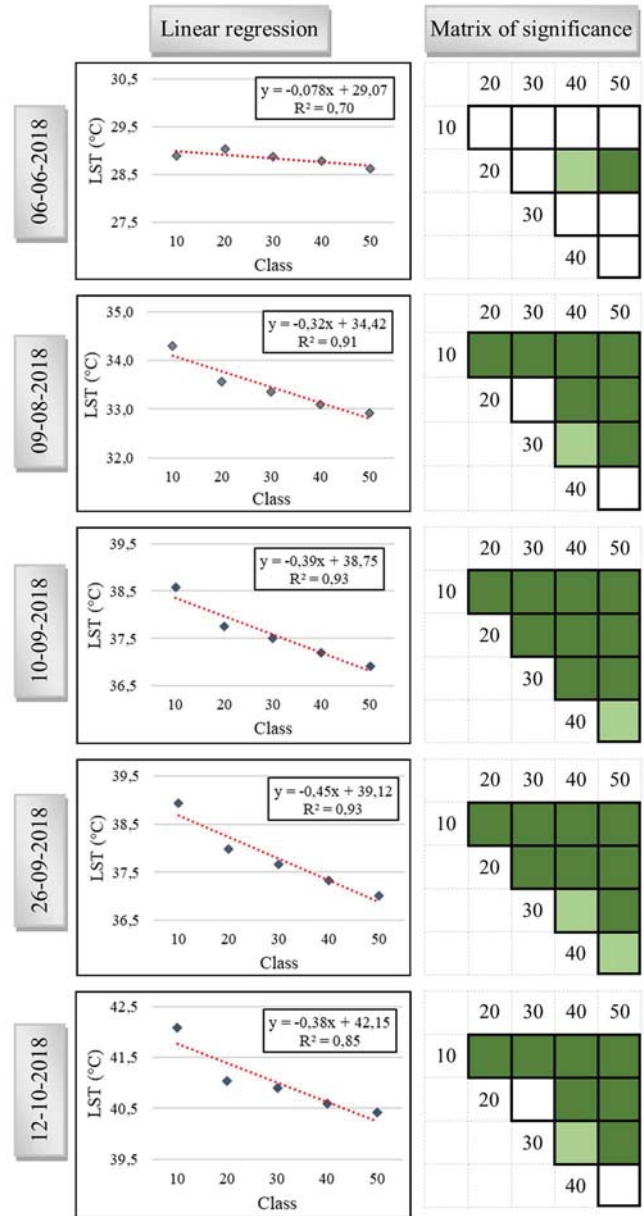


Figure 5: Linear regressions and matrices of significance to the Dunn test of the greenest map for the five dates available, with Land Surface Temperature retrieved with Sentinel 2 scenes. In the matrices, the significant differences between classes are shown in green ($p < 0,01$) and light green ($p < 0,05$).

study of the greenest orthomosaic maps led to improved results. It is possible that the tenfold increase in the number of cells analyzed contributed to reduce the effect of the confounding factors.

A clear temporal pattern was noticed in the analysis of LST, with an increasing trend in temperatures during the dry season. In the early dry season (April – July) calculated LST were lower, sky was cloudier since cloud-free satellite scenes were harder to find, and significant decreases in LST between different TCC classes were not observed. Instead, in the late dry season (August – November) calculated LST were higher, the sky was clearer, and significant results were obtained for the LST/TCC correlation analysis.

One of the reasons that could explain the absence of the LST/TCC correlation in the early dry season is that late crops or pastures, or their residues, might still be covering the soils, and their LST are generally lower compared to bare soils. The other important reason that can be individuated is related to the surface energy balance dynamics, and to the fact that during the early dry season soil moisture contents are likely to be higher. Therefore, more energy contributes to the latent heat flux and less to the sensible heat flux.

The LST temporal pattern and the significative results observed during the late dry season indicated also that trees have an increased impact with higher temperatures.

Further research is needed to define a TCC threshold to be set as objective for ecosystem restoration activities of agricultural landscapes. From our preliminary analyses and considerations, we suggest that a 10% TCC threshold should be reached to have an ameliorated microclimate, in terms of temperature, in this agroecological zone. Considering an average tree crown diameter of 5 meters, the tree density needed to achieve the 10% TCC is 50 trees per hectare, that can also be used as an operative threshold for the RDP.

REFERENCES

- [1] H. J. Mongi, "Addressing Land Degradation in Tanzania: Contemporary Issues Related to Policies and Strategies", 2012. Available at SSRN: <https://ssrn.com/abstract=2150752>
- [2] S. Schnell, C. Kleinn and G. Ståhl, "Monitoring trees outside forests: a review". *Environmental Monitoring and Assessment*, vol. 187:600, 2015. doi: 10.1007/s10661-015-4817-7
- [3] M. Brandt, C. J. Tucker, A. Kariryaa, K. Rasmussen, C. Abel, J. Small, J. Chave, L. V. Rasmussen, P. Hiernaux, A. A. Diouf, L. Kergoat, O. Mertz, C. Igel, F. Gieseke, J. Schöning, S. Li, K. Melocik, J. Meyer, S. Sinno, E. Romero, E. Glennie, A. Montagu, M. Dendoncker, R. Fensholt, "An unexpectedly large count of trees in the West African Sahara and Sahel". *Nature*, 2020. doi: 10.1038/s41586-020-2824-5
- [4] J. Reed, J. van Vianen, S. Foli, J. Clendenning, K. Yang, M. MacDonald, G. Petrokofsky, C. Padoch, and T. Sunderland, "Trees for life: The ecosystem service contribution of trees to food production and livelihoods in the tropics". *Forest Policy and Economics*, vol. 84, pp. 62–71, 2017. doi: 10.1016/j.forpol.2017.01.012
- [5] G. Schroth, and J. A. McNeely, "Biodiversity conservation, ecosystem services and livelihoods in tropical landscapes: Towards a common agenda". *Environmental Management*, vol. 48, pp. 229–236, 2011. doi: 10.1007/s00267-011-9708-2
- [6] S. Kuyah, I. Öborn, M. Jonsson, A. S. Dahlin, E. Barrios, C. Muthuri, A. Malmer, J. Nyaga, C. Magaju, S. Namirembe, Y. Nyberg and F. L. Sinclair, "Trees in agricultural landscapes enhance provision of ecosystem services in Sub-Saharan Africa", *International Journal of Biodiversity Science, Ecosystem Services & Management*, vol. 12:4, pp. 255–273, 2016. doi: 10.1080/21513732.2016.1214178
- [7] T. Shiferaw Sida, F. Baudron, K. Hadgud, A. Dereroe, and K. E. Giller, "Crop vs. tree: can agronomic management reduce trade-offs in tree-crop interactions?" *Agriculture, Ecosystems and Environment*, vol. 260, pp. 36–46, 2018. doi: 10.1016/j.agee.2018.03.011
- [8] J. M. Boffa, "Agroforestry parklands in sub-Saharan Africa." *FAO Conservation Guide* 34, 1999
- [9] M. R. Rao, P. K. R. Nair, and C. K. Ong, "Biophysical interactions in tropical agroforestry systems", *Agroforestry Systems*, vol. 38, pp. 3–50, 1998. doi: 10.1007/978-94-015-9008-2_1.
- [10] S. R. Gliessman, "Agroecology: The Ecology of Sustainable Food Systems" Third Edition. CRC Press Taylor & Francis Group, 2015.
- [11] R. D. Brown, "Ameliorating the effects of climate change: modifying microclimates through design", *Landscape and Urban Planning*, vol. 100, pp. 372–374, 2011. doi: 10.1016/j.landurbplan.2011.01.010.
- [12] D. Ismail, D. Wiegant, E. Hagos, F. van Steenbergen, M. Kool, F. Sambalino, G. Castelli, E. Bresci, and F. Hagos, "Managing the Microclimate." Practical note 27, Spate Irrigation Network Foundation, 2016.
- [13] G. Castelli, F. Castelli, and E. Bresci "Mesoclimate regulation induced by landscape restoration and water harvesting in agroecosystems of the horn of Africa", *Agriculture, Ecosystems and Environment*, vol. 275, pp. 54–64, 2019. doi: 10.1016/j.agee.2019.02.002
- [14] Z. L. Li, B. H. Tang, H. Wu, H. Ren, G. Yan, Z. Wan, I. F. Trigo, and J. A. Sobrino, "Satellite-Derived Land Surface Temperature: Current Status and Perspectives." *Remote Sensing of Environment*, vol. 131, pp 14–37, 2013 doi: 10.1016/j.rse.2012.12.008
- [15] B. B. Lin, "Agroforestry management as an adaptive strategy against potential microclimate extremes in coffee agriculture", *Agricultural and Forest Meteorology*, vol. 144, pp. 85–94, 2007. doi: 10.1016/j.agrformet.2006.12.009
- [16] J. Rogan, M. Ziemer, D. Martin, S. Ratick, N. Cuba, and V. DeLauer, "The impact of tree cover loss on land surface temperature: A case study of central Massachusetts using Landsat Thematic Mapper thermal data", *Applied Geography*, vol. 45, pp. 49–57, 2013 doi: 10.1016/j.apgeog.2013.07.004
- [17] M. Wang, Z. Zhang, T. Hu, and X. Liu, "A Practical Single-Channel Algorithm for Land Surface Temperature retrieval: application to Landsat series data" *Journal of Geophysical Research: Atmospheres*, vol. 124, pp. 299–316, 2019. doi: 10.1029/2018JD029330
- [18] X. Yu, X. Guo, and Z. Wu, "Land Surface Temperature retrieval from Landsat 8 TIRS-comparison between radiative transfer equation-based method, Split Window Algorithm and Single Channel Method." *Remote Sensing* vol. 6, pp. 9829–9852, 2014. doi: 10.3390/rs6109829